J. Membrane Biol. 184, 161–170 (2001)
DOI: 10.1007/s00232-001-0084-3

The Journal of
Membrane
Biology

© Springer-Verlag New York Inc. 2001

Reversible Electropermeabilization of Mammalian Cells by High-Intensity, Ultra-Short Pulses of Submicrosecond Duration

K.J. Müller, V.L. Sukhorukov, U. Zimmermann
Lehrstuhl für Biotechnologie, Biozentrum der Universität Würzburg, Am Hubland, D-97074 Würzburg, Germany

Received: 15 May 2001/Revised: 20 July 2001

Abstract. Mouse myeloma cells were electropermeabilized by single square-wave electric pulses with amplitudes of up to ~150 kV/cm and durations of 10–100 nsec. The effects of the field intensity, pulse duration and medium conductivity on cell viability and field-induced uptake of molecules were analyzed by quantitative flow cytometry using the membrane-impermeable fluorescent dye propidium iodide as indicator molecule. Despite the extremely large field strengths, the majority of cells survived the exposure to ultra-short field pulses. The electrically induced dye uptake increased markedly with decreasing conductivity of the suspending medium. We assigned this phenomenon to the transient electrodeformation (stretching) force that assumes its maximum value if cells are suspended in low-conductivity media, i.e., if the external conductivity σ_e is smaller than that of the cytosol σ_i. The stretching force vanishes when σ_e is equal to or larger than σ_i. Due to their capability of delivering extremely large electric fields, the pulse power systems used here appear to be a promising tool for the electropermeabilization of very small cells and vesicles (including intracellular organelles, liposomes, etc.).

Key words: Electropermeabilization — Electroporation — Conductivity — Myeloma cells — Electroinjection — Flow cytometry

Introduction

Application of high-intensity electric field pulses to freely suspended cells generates a critical transmembrane voltage, which leads to a drastic increase in permeability of the plasma membrane once the breakdown voltage is exceeded. It is generally accepted that membrane breakdown occurs if the induced membrane voltage reaches a value of about 1 V at room temperature (Zimmermann, Pilwat & Riemann, 1974). Based on this phenomenon, a wide range of practical applications of pulsed electric fields for the reversible and irreversible permeabilization of cell membranes has been identified in many areas of biotechnology and medicine (Collombet et al., 1997; Heinz et al., 1999; Hofmann et al., 1999; Marzszalek et al., 1997; Zimmermann & Neil, 1996). The most important biomedical application of the reversible electropermeabilization is the electroinjection technique that allows the introduction of membrane-impermeable xenomolecules (such as dyes, hormones, proteins, plasmids, etc.) into living cells (Zimmermann & Neil, 1996; Djuzenova et al., 1996; Gift & Weaver, 2000; Friedrich et al., 1998; Zimmermann et al., 2000). Electroinjection and particularly electrotransfection (i.e., plasmid injection) have gained common acceptance because they are more controllable, reproducible, and efficient than alternative chemical or viral methods (for review *see* Zimmermann & Neil, 1996; Lynch & Davey, 1996).

The degree of membrane electropermeabilization, molecular uptake and cell survival upon electric membrane breakdown depend critically—among other parameters—on the duration of the applied field pulses. Whereas long-duration pulses of the millisecond range are generally well tolerated by bacteria, which are protected by strong cell walls, much shorter field pulses are usually required to avoid the irreversible membrane breakdown and excessive lysis of fragile eukaryotic cells, such as mammalian cells and isolated plant or yeast protoplasts (Zimmermann & Neil, 1996). Thus, the survival of electrotransfected mammalian cells from various

Correspondence to: U. Zimmermann; e-mail: zimmermann@biozentrum.uni-wuerzburg.de

cell lines is substantially improved if short field pulses with the duration of 10–100 μsec are applied (Friedrich et al., 1998). It can therefore be expected that the use of ultra-short pulses of submicrosecond durations could further enhance survival of eukaryotic cells after electric-field treatment. However, conventional pulse generators (including commercial devices) are not able to produce sub-μsec pulses of field strengths sufficient for electropermeabilization of cell membranes.

Recently, both theoretical and experimental studies have shown (Isambert, 1998; Sukhorukov, Mussauer & Zimmermann, 1998) that the electro-deformation force imposed on the cell during the time course of the pulse can contribute greatly to electropermeabilization of mammalian cells. The electro-deformation force is caused by the Maxwell stress at membrane interfaces and can also be viewed as a result of electrostatic interaction between the induced cell dipole and the applied field. Under low-conductivity conditions, electro-deformation (electrostretching) stress promotes enlargement of the permeabilized membrane area. Whereas membrane charging and breakdown occur on the time scale of about 1 μsec for typical mammalian cells, the transient electro-deformation force is much faster and arises in the nsec-time range (Mussauer, Sukhorukov & Zimmermann, 1999; Zimmermann et al., 2000). Until now, the time resolution required for studying the electro-deformation response of living cells could only be achieved by frequency-domain techniques using alternating (AC) fields (Engelhardt & Sackmann, 1988; Pawlowski & Fikus, 1989; Krueger & Thom, 1997; Sukhorukov et al., 1998; Kononenko & Shimkus, 2000). However, AC electro-deformation experiments are restricted to relatively low driving voltages supplied by high-frequency generators.

The use of high-intensity DC pulses with durations shorter than the time constant of membrane charging can therefore offer valuable insight into the biophysical mechanisms involved in electropermeabilization of cells. The technical advance in the field of pulsed-power equipment (Kristiansen & Hagler, 1987; Küchler, 1996; Schoenbach et al., 1997) enabled this study, in which the efficiency of ultra-short electric pulses for the reversible permeabilization of mammalian cell membranes was examined. To this end, pulse generators were built that were capable of delivering square-wave pulses with voltages of up to ~15 kV and durations between 10 and 100 nsec. Mouse myeloma cells were exposed to these ultra-short pulses, and the degree of electropermeabilization and viability of cells was quantified by spectrofluorimetry and flow cytometry using the fluorescent dye propidium iodide (PI) as the indicator molecule. Under optimum conditions, the ultra-short pulses induced considerable dye uptake without significant loss of cell viability. The electrically driven uptake of PI induced by ultra-short pulses was comparable to that obtained with conventional pulses of 20–40-μsec duration and reasonable field strengths (about 3 kV/cm), but application of nsec-pulses required much larger field intensity of up to ~150 kV/cm. As with μsec-pulses (Sukhorukov et al., 1998), the molecular uptake induced by ultra-short pulses increased markedly with decreasing medium conductivity, indicating that under low-conductivity conditions the electromechanical stretching force promotes the enlargement of "electropores" in the cell membrane generated by electric breakdown.

Materials and Methods

Cells

The murine myeloma cell line Sp2 was cultured in RPMI 1640 complete growth medium containing 10% FCS (fetal calf serum, PAA, Linz, Austria) at 37°C under 5% CO_2. The cells were kept in the exponential growth phase by passaging three times weekly. The cells were washed 1–2 times with and resuspended in pulse medium 10 min before electrical pulsing.

Electroinjection of Propidium Iodide

Pulse media contained 0.85 mM K_2HPO_4, 0.3 mM KH_2PO_4 (pH 7.4) and either 7, 16, 25, 30 or 35 mM KCl with corresponding conductivities of about 1, 2, 3, 4 or 5 mS/cm at 22°C. The osmolality of the media was adjusted to 290 mOsm by addition of appropriate amounts of inositol (I-5125; Sigma, St. Louis, MO). Conductivity and osmolality were measured by means of a conductometer (Knick, Berlin, Germany) and a cryoscope (Osmomat 030, Gonotec, Berlin, Germany), respectively.

The experimental protocol for electroinjection of PI into cells included the foll
owing steps: (1) suspension of cells at a final cell density of $1–2 \times 10^6$ cells/ml in pulse media containing 25 μg/ml PI (Sigma, P-4170; aqueous stock solution 1 mg/ml); (2) application of a single electric field pulse to cell samples (100 μl) at room temperature (22–24°C) using the pulse generators and cuvettes described below; (3) resealing, i.e., post-pulse incubation of cells in the pulse medium, for 10 min at 22–24°C. Under these conditions, the time constant of the membrane resealing is about 2 min (Sukhorukov et al., 1995), i.e., considerably longer compared to 37°C (Zimmermann & Neil, 1996); (4) within 10–15 min after pulse application PI staining of cells was analyzed by flow cytometry or spectrofluorimetry.

Nanosecond-Pulse Generators

In this study, two different pulsers for generation of ultra-short square-wave pulses were built in a circuit category of pulse-forming network (PFN). The design and construction of the pulse generators consisting of a distributed transmission line as PFN are described in detail elsewhere (Kristiansen & Hagler, 1989; Schoenbach et al., 1997). The pulse width of these generators is determined by the length (L) of their transmission lines. The first pulser used here consisted of a strip line ($L \approx 1$ m) as PFN, which was capable of supplying a defined, invariable pulse width of 11 ± 0.1 nsec. Longer pulses were generated by means of a PFN consisting of several coaxial cables in parallel. The use of replaceable cables of various length ($L \approx 3$, 5, or 9 m) enabled this PFN

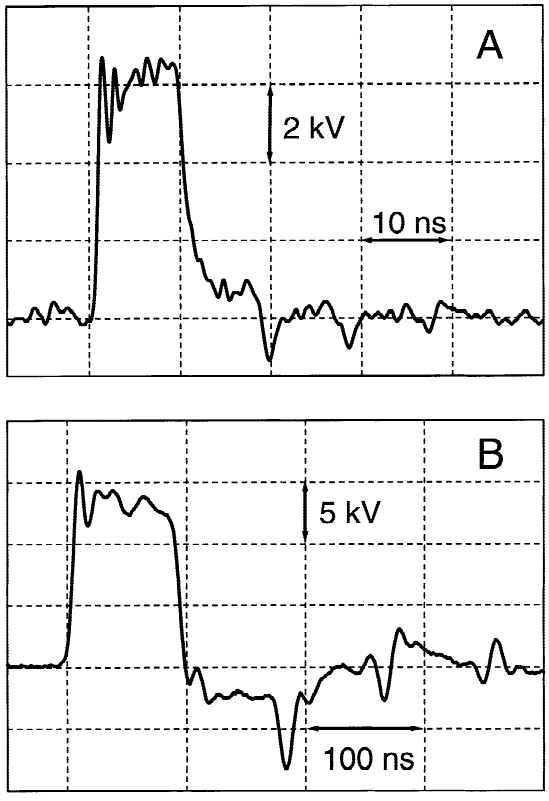

Fig. 1. Typical discharge pulses supplied by the strip-line (*A*) and cable pulsers (*B*). The strip-line system generates high-voltage square-wave pulses with 10 nsec duration (*A*). The cable system, equipped with five coaxial cables of 9 m length each, yields pulses with 95 nsec duration (*B*).

to produce pulse widths of about 45, 65 and 95 nsec, respectively. Both pulsers could be charged up to about 30 kV by means of a DC power supply (HCN 350–35000, FUG, Rosenheim, Germany). Charging was completed when the voltage of the PFN was equal to that of the power supply. The energy stored in the PFN capacitance was discharged into a matched load (*see* below) by means of a closing switch that was designed as a spark gap operating in the self-breakdown mode. The load consisted of a high-voltage resistor connected in parallel with a cuvette filled with the cell suspension (100 μl). The cuvettes consisted of two plane aluminum electrodes (1 cm^2 area) spaced by 1 mm (Friedrich et al. 1998).

The pulse voltage V_0 across the cell sample was monitored online by means of a 500-MHz digital storage oscilloscope (Tektronix, TDS 3052, Wilsonville, OR) connected to the pulsing cuvette. Typical pulse shapes are illustrated in Fig. 1. From these signals, the field strength E_0 applied to the cell sample was calculated as $E_0 = V_0/d$, where d is the distance between the electrodes. With a distance of 1 mm, the maximum field strength of about 150 kV/cm could be obtained for the strip-line as well as for the cable pulser.

Electropermeabilization Using Microsecond Pulses

In a parallel set of experiments, the Multiporator distributed by Eppendorf (Hamburg, Germany) was used for electropermeabilization. This instrument generates exponentially decaying field pulses with peak intensities of up to 1.2 kV and decay times between 15 and 500 μsec. The main advantage of the Multiporator is its ability to deliver high-voltage pulses whose duration is controlled by a microprocessor unit. This electronic enhancement ensures high reproducibility of the pulsing conditions regardless of any variations in the ionic content of the pulse media, including changes in the medium conductivity that can arise because of ion leakage from the cytosol or of cell lysis that may occur during pulse application (Friedrich et al., 1998).

Determination of PI Uptake

Measurements of PI uptake were performed in a flow cytometer Epics XL system (Beckman Coulter, Fullerton, CA) equipped with a 15-mW 488-nm argon-ion laser. Cellular red fluorescence (RF) signals from samples containing about 5000 cells were acquired in logarithmic mode using the band pass filter 675 ± 5 nm. The output RF data were shown as one-dimensional histograms representing distributions of the intracellular dye. The content of internalized PI [fmol/cell] and cell viability in electropulsed cell samples were evaluated from RF-histograms as described elsewhere (Sukhorukov et al., 1995; Djuzenova et al., 1996).

Measurements of electrically induced PI uptake were also carried out by spectrofluorimetry. Ten minutes after electropulsing, cell samples (100 μl) containing 25 μg/ml PI were diluted with 2 ml phosphate-buffered saline. The fluorescence spectra of cell suspensions in a wavelength range from 560 to 660 nm were measured by means of a Perkin-Elmer fluorimeter (model LS-50) upon excitation at 535 nm. Fluorescence intensity values for the maximum PI uptake were obtained by adding 0.2% saponin, which induced complete membrane permeabilization. The number of viable cells was also determined before and after pulse administration by electronic cell counting using a CASY-1 instrument (Schärfe Systems, Reutlingen, Germany).

Deformation of Cells by an AC Electric Field

AC-electrodeformation of cells was observed under low-conductivity conditions using a microstructure that had been fabricated photolithographically at the Fraunhofer-Institut Siliziumtechnologie (ISiT, Itzehoe, Germany). It consisted of a planar array of four parallel sawtooth-shaped microelectrodes of interdigitated geometry. The electrode fingers were 140 nm thick (20 nm Ta and 120 nm Pt) and 100 μm long. The distance between two opposite electrode tips was 30 μm. A sample of cell suspension (50–70 μl, about 3×10^5 cells/ml) was added to the electro-deformation chamber, and a coverslip was placed gently over its center. After cells had settled for about 3 min, a 5-MHz field of about 200 V/cm was applied for 5–10 sec to direct cells to the electrode tips by positive dielectrophoresis. The field was supplied by a function generator TE 7702 (Toellner, Herdecke, Germany). The field strength was then gradually increased to 5 kV/cm and was kept constant for 1–2 min at the same frequency of 5 MHz. The observation of electrodeformation was performed using an Olympus microscope (BX 51, Olympus, Hamburg, Germany) equipped with a high-resolution CCD camera Colorview 12 and a computer-supported image capture system analySIS (Soft Imaging System, Münster, Germany).

Results

Fluorimetry of Cell Suspensions

The fluorescence spectra of cell suspensions presented in Fig. 2 illustrate the effects of electric pulses of various

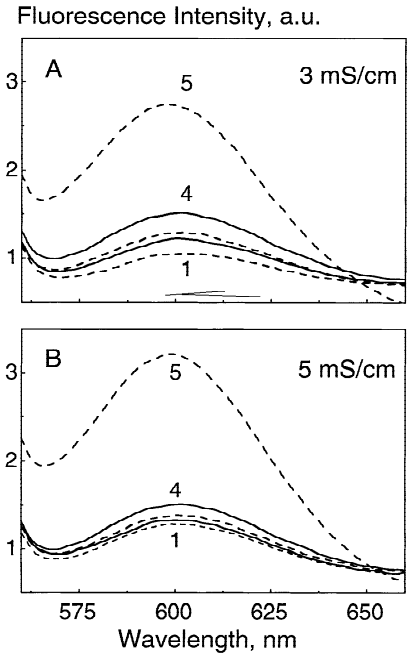

Fig. 2. Typical fluorescence spectra of PI in control (curves *1*), electropulsed (curves *2–4*) and saponin-lyzed (curves *5*) cell suspensions. Cells (10^6/ml, 100 μl) suspended in isotonic pulse media of conductivity 3 and 5 mS/cm (*A* and *B*, respectively) were exposed to a single 95-nsec pulse of 125, 153 and 165 kV/cm strength at room temperature (curves *2*, *3* and *4*, respectively). Ten minutes after electroporation, the cell samples were diluted with 2 ml phosphate-buffered saline and their fluorescence spectra were measured upon excitation at λ_{ex} = 535 nm.

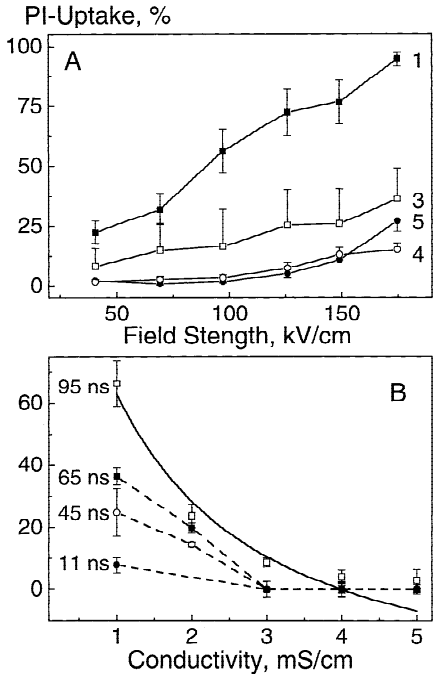

Fig. 3. Field strength (*A*) and conductivity (*B*) dependence of the electrically induced PI-staining of Sp2 cells. Fluorescence spectra of cell suspensions such as shown in Fig. 2 were used to quantify the electrically driven PI uptake expressed as the percentage of red fluorescence (λ_{em} = 600 nm) of saponin-lysed cell samples (*see* Text). In *A*, the cells were exposed to single pulses of different strengths (E_0 = 40–160 kV/cm) but of the same duration of 95 nsec. In *B*, single pulses of a constant intensity E_0 of 160 kV/cm with a duration of 11, 45, 65 or 95 nsec were applied. In *A* and *B*, the numbers near the symbols indicate the medium conductivity in mS/cm and the pulse duration in nanoseconds, respectively. The datapoints are the means with standard errors of 3–9 determinations. The solid curve in *B* show the best fit of the normalized electro-deformation force $F_D \propto (\sigma_i^2 - \sigma_e^2)/(\sigma_i + 2\sigma_e)^2$ (*see* Eq. 5) to the data obtained with the 95-nsec pulser, assuming σ_i = 4 mS/cm.

field strengths on the electroinjection of PI. Pulses with the duration of 95 nsec were supplied by the cable pulser. Electropulsing was performed at two different conductivities of 3 and 5 mS/cm (Figs. 2*A* and 2*B*, respectively). The PI fluorescence spectra of the unpulsed controls (curves *1*) and of saponin-lysed cell samples (curves *5*) are also shown. Saponin-lysed (dead) cells showed a very bright red fluorescence due to the rapid equilibration with the 25 μg/ml PI present in the medium. With increasing field strength of the nsec-pulse (curves *2–4*), the intensity of PI fluorescence increased gradually, indicating a higher degree of membrane permeabilization responsible for the dye uptake. Note that the fluorescence intensity of electropulsed samples was much smaller than that of saponin-lysed cells, indicating that under these field conditions there was no saturation of the cellular binding sites for PI. It is also evident from Fig. 2 that an increase of medium conductivity from 3 to 5 mS/cm resulted in a marked decrease of the amount of electroinjected PI.

The fluorescence spectra of electropulsed cell suspensions as shown in Fig. 2 were used to quantify the electro-uptake of the dye. PI uptake was expressed as the percentage of red fluorescence in saponin-lysed cell samples: PI uptake = $(F_{EP} - F_0)/F_{SAP} \times 100\%$, where F_{EP}, F_0, and F_{SAP} are the fluorescence intensity values at λ = 598 nm of electropulsed, untreated control and saponin-lysed cell samples, respectively. The PI uptake data as function of the field strength and of the conductivity of the pulse medium are summarized in Fig. 3. It is evident that PI staining increased with increasing field strength (Fig. 3*A*) and decreasing medium conductivity (Figs. 3*A* and *B*). In the experiments shown in Fig. 3*B*, the field strength was kept constant at E_0 = 160 kV/cm. At a pulse duration of 95 nsec, the PI uptake decreased sharply from 66 ± 7% to 9 ± 2% as the conductivity σ_e was increased from 1 to 3 mS/cm, respectively. In more conductive media (4 and 5 mS/cm), the electrically induced uptake was very low (~3–4%) at E_0 = 160 kV/cm (Fig. 3*B*) and hardly detectable at field strengths less than 125 kV/cm (curves *4* and *5* in Fig. 3*A*). The use of shorter pulses with durations of 65, 45 and 11 nsec (Fig. 3*B*) gave lower dye uptake but the corresponding conductiv-

ity dependence was qualitatively similar to that obtained with 95 nsec duration pulses.

Although spectrofluorimetry is useful for the quantitative evaluation of electropermeabilization, this method yielded only PI uptake values averaged over the whole cell population. Furthermore, it did not permit the discrimination between reversibly (live) and irreversibly (dead) permeabilized cells. In contrast, assessment of PI-stained cells by flow cytometry is an alternative approach to studying the responses of various subpopulations of cells to electric field treatment (Sukhorukov et al., 1995).

Flow Cytometry

Typical RF distributions of electropulsed, untreated control and saponin-lyzed Sp2 cells suspended in pulse medium of conductivity 3 mS/cm are shown in Fig. 4. The histogram of untreated cells in the absence of PI (Fig. 4*B*, curve *0*) exhibited a very weak autofluorescence peak centered at about 2 arbitrary units (a.u.). After the addition of 25 μg/ml PI, this peak shifted slightly to 4–5 a.u. (curves *1* in Figs. 4*A* and *B*), which was obviously due to the adsorption of the membrane-impermeable dye to the outer membrane surface. Usually, only a small fraction (< 5%) of unpulsed cell samples showed RF intensities larger than 300 a.u. after the staining with PI. This subpopulation consists of dead cells, as demonstrated by the addition of 0.2% saponin. Saponin-treated cells showed a very high RF intensity level ranging from about 300 to 1000 a.u. (curve *S* in Fig. 4*B*), which corresponded to near saturation of the intracellular binding sites for PI (Sukhorukov et al., 1995).

The PI content distributions in electropulsed cell samples (Fig. 4*A*, curves *2–5* and Fig. 4*B*, curves *2–3*) differed markedly from those observed in control and saponin-lysed cell cultures. Independent of the pulse generator used, exposure of cells to a field pulse in the presence of PI led to the appearance of two readily distinguishable subpopulations: a) irreversibly permeabilized dead cells with very bright RF (centered at 700–800 a.u.) similar to that of the saponin-lysed samples, and b) cells with much lower PI staining (4 < RF < 300 a.u.), i.e., being far from equilibrium with the medium. This subpopulation consisted of transiently permeabilized, viable cells. As expected, the ultra-short pulses (Fig. 4*A*) required much larger field strengths in order to achieve PI staining than did the conventional μsec-pulses (Fig. 4*B*). Thus, to obtain a PI-uptake level of 60–70 a.u. achieved with a pulse of 40 μsec duration and 2 kV/cm intensity (curve *2*, Fig. 4*B*), the 95-nsec pulse required a field strength of about 150 kV/cm (curve *5* in Fig. 4*A*). Note that the percentage of strongly fluorescent, dead cells (RF > 300 a.u.) produced by both pulse systems was very low (about 5%) indicating that in both cases the majority of electropermeabilized cells was able to recover its original membrane impermeability within few minutes after electropulsing. This was also confirmed by electronic cell counting (*data not shown*).

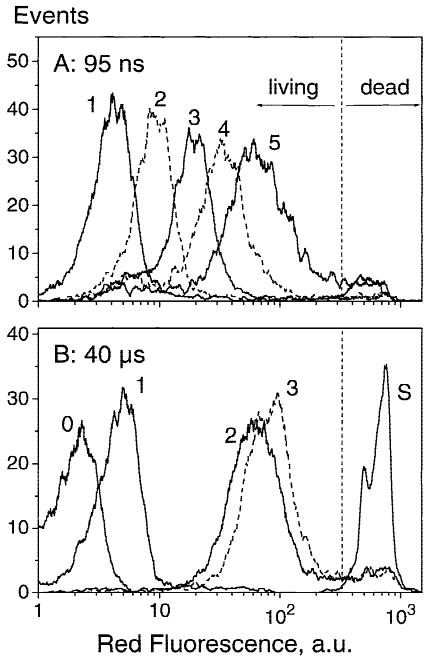

Fig. 4. Representative histograms of PI-DNA fluorescence of control and electropulsed Sp2 cells. Measurements were performed 10–15 min after electropulsing in the presence of 25 μg/ml PI. (*A*) Curve *1* shows the RF signals of unpulsed control cells in the presence of PI; histograms *2, 3, 4* and *5* represent cell samples exposed to a single 95-nsec pulse with field strengths of 74, 93, 125 and 150 kV/cm, respectively, in the presence of PI. The 95-nsec pulses were generated by means of the cable-type pulser (*see* Material and Methods). (*B*) Curves *0* and *1* show the autofluorescence of cells in the absence and presence of 25 μg/ml PI, respectively; curve *S* represents saponin-treated cells in the presence of PI; histograms *2* and *3* represent cell samples exposed to a single 40-μsec pulse with field strengths of 2 and 3 kV/cm, respectively, generated by means of the Eppendorf-Multiporator. Note that, independent of the pulse system used, only a small fraction of cells (about 5%) was irreversibly permeabilized (dead).

The flow-cytometric RF histograms, such as shown in Fig. 4, allowed the quantification of the intracellular PI content in electropulsed living cells. Because of the relatively broad RF-distributions the modal RF signal was used as a measure for the dye uptake by living cells. The strongly fluorescent lysed cells, whose RF signal corresponds to about 10 fmol PI per mean Sp2 cell (Sukhorukov et al., 1995), were used as the internal standard of the intracellular dye content.

The effects of field pulses of various strengths and durations on the amount of electroinjected PI are shown in Fig. 5. For the ultra-short pulses (e.g., 95 nsec, Fig. 5*A*), measurable PI uptake was observed at field intensities larger than 40 kV/cm. For field intensities of up to 100 kV/cm, curve fitting revealed a strictly quadratic

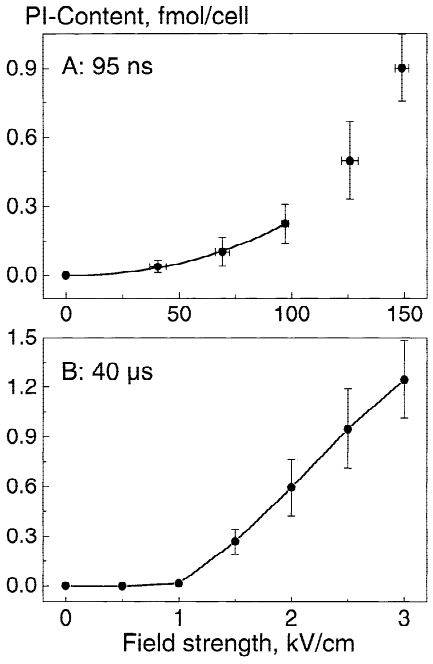

Fig. 5. Dependence of the electrically induced PI uptake on the applied field strength E_0 at a constant pulse duration of 95 nsec (*A*) and 40 µsec (*B*). Electropulsing was performed at a conductivity of 2.5 mS/cm. The mean PI content in living cells was evaluated from RF histograms as shown in Fig. 4. Each symbol represents the mean ±SEM from 3–4 independent flow cytometric determinations. The continuous curve in *A* shows the best fit of the function $y = ax^b$ to the data obtained at E_0 <100 kV/cm with the exponent $b = 2.1 \pm 0.1$ (±SEM of fitting).

dependence of the PI uptake on the applied field strength upon application of the ultra-short pulses (solid curve in Fig. 5*A*). In the case of 40-µsec pulses, a progressive increase of PI uptake was observed above a threshold field strength near 1 kV/cm (Fig. 5*B*). It is noteworthy, that this experimental value is close to the theoretical threshold $E_{crit} = 950$ V/cm estimated from the steady-state equation for the induced membrane potential V_g at the cell poles facing the electrodes (*see* Discussion).

Discussion

The theory of electropermeabilization of cells upon membrane charging is given in full detail elsewhere (Zimmerman and Neil, 1996). We have recently shown (Sukhorukov et al., 1998; Zimmermann et al., 2000) that the electromechanical stretching force on the cell membrane must be taken into account additionally to membrane charging in order to explain the strong conductivity-dependence of the electrically induced dye uptake. Electrodeformation of cells and related electrokinetical phenomena were treated theoretically elsewhere (Winterhalter & Helfrich, 1988; Pawlowski & Fikus, 1989; Hyuga, Kinosita & Wakabayashi, 1991; Kinosita et al., 1992; Jones, 1995; Zimmermann & Neil, 1996; Pethig & Markx, 1997; Isambert, 1998). Thus, we will only consider the basic assumptions and equations useful for the interpretation of the results obtained in this study.

Table 1. Numeric values of some parameters important for the electropermeabilization of Sp2 cells at the various conductivities of the suspending medium used in these study

σ_e mS/cm	τ_m nsec	τ_i nsec	T_B nsec		P_D kP_a	
			$E_0 = 3$ kV/cm	100 kV/cm	3 kV/cm	100 kV/cm
1	525	3.5	201	5.0	0.12	133*
2	350	2.7	134	3.3	0.05	60
3	292	2.1	112	2.8	0.02	22
4	263	1.8	100	2.5	0	0
5	245	1.5	94	2.3	−0.01	−15#

The values of τ_m, τ_i, T_B and P_D were calculated with Eqs. 1, 2, 3, 4, 5, 6 using the electrical parameters of Sp2 cells reported earlier (Kürschner et al., 1998).

* Note that this P_D value of the electrical stretching stress is larger than the compressive electrostatic pressure $P_m = C_m V^2/2$ imposed to a membrane charged to the critical voltage V_C of 1V. Positive and negative P_D values correspond to cell elongation and compression along the field lines, respectively.

For $\sigma_e > \sigma_i = 4$ mS/cm, P_D is negative leading to cell compression in the field direction.

Membrane Charging

In response to an applied DC electric field E_0, the voltage generated across the plasma membrane of a spherical cell grows exponentially with time (Zimmermann & Neil, 1996):

$$V_g(t) = 1.5aE_0 \cos\theta\,(1-\exp(-t/\tau_m)), \quad (1)$$

whereby θ is the polar angle measured with respect to field E_0. The relaxation time constant τ_m of the plasma membrane charging is given by (Jeltsch & Zimmermann, 1979):

$$\tau_m = aC_m\left(\frac{1}{\sigma_i}+\frac{1}{2\sigma_e}\right). \quad (2)$$

As can be seen from Eq. 2, τ_m decreases with increasing external conductivity σ_e, indicating that the membrane charges faster if cells are suspended in a high-conductivity medium. Using the relevant parameters for Sp2 cells, i.e., $a = 7$ µm, $C_m \approx 1$ µF/cm^2 and $\sigma_i \approx 4$ mS/cm reported previously (Kürschner et al., 1998), the τ_m values of 0.25–0.53 µsec were estimated from Eq. 2 for the conductivity range 1–5 mS/cm (Table). Note that these τ_m values are much smaller than the duration of the

20–40 μsec pulses generated by the conventional device. At these pulse durations, and for $t \gg \tau_m$, Eq. 1 simplifies to the well known steady-state expression:

$$V_g = 1.5\, aE_0 \cos\theta \tag{3}$$

In the case of the ultra-short 10–100 nsec pulses, however, the static equation 3 is not applicable because these pulses are shorter than τ_m (Table). Instead, Eq. 1 must be used for estimation of the temporal and spatial distribution of the induced membrane voltage.

As already mentioned, membrane breakdown occurs when V_g reaches its critical value V_C. In this study, electropermeabilization was performed at room temperature, and therefore, V_C of 1V can be assumed. Using the known value for the cell radius ($a = 7$ μm), the critical field strength E_{crit} required for the reversible electric breakdown at the membrane sites facing the electrodes ($\cos\theta = 1$) can be estimated from Eq. 3: $E_{crit} = V_C/(1.5 \times a) = 950$ V/cm. Once the membrane is charged to 1 V, breakdown occurs very quickly, i.e., at the subnanosecond time scale, as shown in experiments on lipid bilayers (Benz, Beckers & Zimmermann, 1979). Upon breakdown, the membrane becomes highly conductive, so that no further increase in V_g can occur, even if the cells are exposed to very high, supracritical fields ($E_0 \gg E_{crit}$) (Kinosita et al., 1992).

The theoretical considerations can explain the strong dependence of the degree of electropermeabilization on both, field strength and pulse duration. However, most current theories do not account for the strong conductivity-dependence of electropermeabilization observed for *n*sec-pulses (Figs. 2 and 3) and for μsec-pulses (Kinosita & Tsong, 1977; Dimitrov & Sowers, 1990; Djuzenova et al., 1996; Mussauer et al., 1999). As discussed below, the transient electrodeformation force acting on the cell might be responsible for the increased molecular uptake observed under low-conductivity conditions.

Transient Cell Polarization

In addition to membrane charging discussed above, the applied field generates a dipole within the cell. The induced-dipole moment μ_c is proportional to the field strength E_0 and to the effective polarizability of the cell U_c relative to the suspending medium (Stenger, Kaler & Hui, 1991; Jones, 1995; Zimmermann & Neil, 1996; Pethig & Markx, 1997; Fuhr et al., 1998):

$$\mu_c(t) = 4\pi\varepsilon_e\varepsilon_0 a^3 E_0\, U_C(t) \tag{4}$$

After application of a DC pulse, the dipole μ_C varies with time in a quite complicated manner. The dipole is first given by $U_{C1} = (\varepsilon_i - \varepsilon_e)/(\varepsilon_i + 2\varepsilon_e) \approx 0$ (because $\varepsilon_i \approx \varepsilon_e$), then by the intermediate value $U_{C2} = (\sigma_i - \sigma_e)/(\sigma_i + 2\sigma_e)$ and finally by U_{C3}. The polarizability factor U_{C3} depends on the conductivity of the plasma membrane G_m ($= \sigma_m/d$). At low field strengths (i.e., $E_0 < E_{crit} \approx 1$ kV/cm), the plasma membrane remains insulating ($\sigma_m \to 0$) and the effective cell polarizability is given by $U_{C3} \approx (a\, G_m - \sigma_e)/(a\, G_m + 2\sigma_e) \approx -0.5$ (Jones, 1995; Sukhorukov et al., 1998). However, at supracritical field strengths $E_0 \gg E_{crit}$, such as used for electropermeabilization, the cell membrane undergoes breakdown and becomes highly conducting. In this case, the following relation $U_{C3} = U_{C2} = (\sigma_i - \sigma_e)/(\sigma_i + 2\sigma_e)$ is valid as long as the external field is on, providing that σ_m has been increased to a value larger than $\sigma_i\sigma_e/(\sigma_i - \sigma_e)$.

The transition $U_{C1} \to U_{C2}$ occurs very fast with the time constant of the cytosol polarization τ_i given by (Jones, 1995):

$$\tau_i = \frac{\varepsilon_i + 2\varepsilon_e}{\sigma_i + 2\sigma_e} \tag{5}$$

Using appropriate values for Sp2 cells, i.e., $\varepsilon_i \approx \varepsilon_e \approx 80\ \varepsilon_0$, and $\sigma_i = 4$ mS/cm (Kürschner et al., 1998), the τ_i values of 1.5–3.5 nsec were calculated from Eq. 5 for the range of external conductivity used in this study (Table). Note that τ_i is smaller than τ_m by at least two orders of magnitudes.

Transient Electro-deformation Force

As already mentioned, the electrostatic interaction between field E_0 and dipole μ_C results in the electrodeformation force F_D acting on the cell membrane. The time course of F_D in response to a DC field pulse is similar to that of the induced dipole. After a short transient regime of the time scale of the cytosolic polarization, i.e., $\tau_i \approx 1$–3 nsec (Eq. 5, Table), the radial electric pressure P_D acting on the plasma membrane reaches a steady value, which can be given by the following approximation (Taylor, 1966; Isambert, 1998):

$$P_D = \frac{9}{2}\varepsilon_e\varepsilon_0 E_0^2 \cos^2\theta \frac{(\sigma_i^2 - \sigma_e^2)}{(\sigma_i + 2\sigma_e)^2} \tag{6}$$

Equation 6 was obtained from the general expression for the radial electric stress (*see* Eq. 9 in Taylor, 1966) by assuming that $\varepsilon_i = \varepsilon_e$. As can be seen from Eqs. 4 and 6, the sign (i.e., the direction) of both μ_C and P_D is determined only by the ratio σ_i/σ_e. Thus, for $\sigma_e < \sigma_i$, the electrodeformation force tends to elongate the cell along the direction of the applied field. In contrast, cells suspended in a high-conductivity medium ($\sigma_e > \sigma_i$) are compressed by the field. In the special case of $\sigma_e = \sigma_i$, the electro-deformation force vanishes. Equation 6 corresponds to the intermediate dipole state U_{C2} given by $(\sigma_i - \sigma_e)/(\sigma_i + 2\sigma_e)$ dominated by the cytosolic polarization (*see* above), so that both quantities P_D and U_{C2} show

similar dependence on σ_e. (For an insulating membrane, i.e., for small electric fields at which $\sigma_m \approx 0$, Eq. 6 is valid only within a very short time interval *t*, satisfying the conditions $\tau_i < t \ll \tau_m$.)

The pressure P_D given by Eq. 6 is applied to one side of the cell membrane, whereas the compressive electrostatic stress P_m related to membrane charging $P_m = C_m \times V_g^2/2$ is imposed on both membrane sides (Zimmermann et al., 1974). The substitution of V_g by $V_C = 1V$ yields a critical P_m value of about 90 kPa ≈ 1 bar, which can be viewed as the mechanical counterpart of the breakdown voltage V_C. Note that the electro-deformation pressure P_D can produce comparable mechanical stresses on the cell membrane without charging, providing that the cell is exposed to very large field intensities (*see* Table).

Equation 6 is identical to the expression derived by Taylor (1966) for a homogeneous drop of conductivity σ_i (without membrane separation) suspended in a conducting fluid (σ_e), on condition that $\varepsilon_e = \varepsilon_i$. Therefore, Eq. 6 also holds for electropermeabilized cell membranes, providing that the electric breakdown has substantially increased σ_m. For strong electric field pulses such as used in this study (e.g., $E_0 = 100$ kV/cm), the membrane breakdown occurs within a very short time $T_B \approx 2.3$–5 nsec after field application (Table). These T_B values are obtained from Eq. 1 by equating the induced membrane voltage V_g with the critical value $V_C = 1$ V required for electropermeabilization: $T_B = -\tau_m \ln(1 - V_C/1.5aE_0)$. The estimated T_B values are (much) smaller than the durations of the applied field pulses, so that, under low-conductivity conditions, the electrical stretching force on the cell is operational as long as the external DC field is on.

It is interesting to note that Eq. 6 is also valid for cells subjected to an AC electric field of a sufficiently high frequency (typically 1–10 MHz). At these field frequencies, the plasma membrane is capacitively bridged, and the cytosolic conductivity determines the electro-deformation response of the cell (Engelhardt & Sackmann, 1988; Kinosita et al., 1992; Sukhorukov et al., 1998). The AC electro-deformation response of Sp2 cells is illustrated in Fig. 6. Under low-conductivity conditions ($\sigma_e = 1$ mS/cm), a steady elongation of the cell in the field direction was observed upon application of a 5-MHz field ($E_0 = 5$ kV/cm). This field frequency corresponds to the time range $t \approx (2\pi f)^{-1} \approx 27$ nsec. The difference between the stationary electro-deformation force due to a constant AC field and the transient deformation force during DC pulse application is discussed in detail elsewhere (Sukhorukov et al., 1998).

According to Eq. 6, the electro-deformation stress P_D acting on the membrane increases with increasing field strength E_0 and decreasing medium conductivity σ_e. The table summarizes the estimated values for P_D induced at the cell poles in the radial direction parallel to the field ($\cos\theta = 1$). Thus, at $E_0 = 100$ kV/cm and $\sigma_e = 1$ mS/cm, the cell membrane experiences an elongation pressure of 133 kPa, which is even larger than the maximum electrostatic compressive stress on the membrane charged to the critical breakdown voltage $V_C = 1$ V ($P_m = 90$ kPa). Unlike the compressive stress P_m imposed on both sides of the membrane, the electro-deformation stress P_D is applied only to one side of the membrane, thus leading to cell elongation (or compression) in the direction parallel to the field lines.

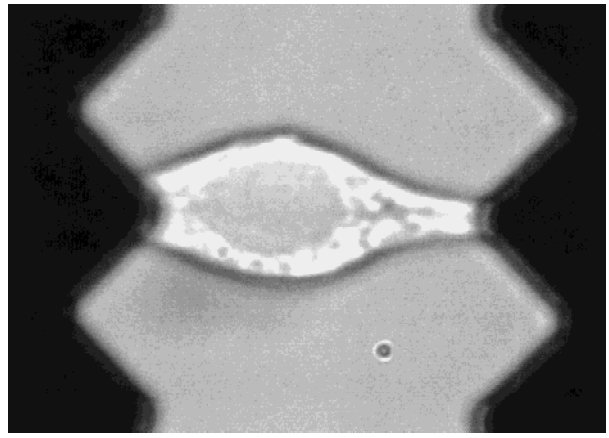

Fig. 6. Deformation of a mouse myeloma cell exposed to a AC field of 5 MHz frequency and 5 kV/cm strength in a low-conductivity solution of 1 mS/cm. The linear AC field was produced within a planar microelectrode structure with an interdigitated geometry. The distance between the tips of the neighboring electrodes is 30 μm.

Conductivity Dependence of Electropermeabilization

The results presented in Figs. 2 and 3 show the effect of the conductivity of the pulse medium σ_e on the incorporation of PI into mouse myeloma cells induced by the ultra-short electric pulses. It is evident that the PI uptake was much larger in low-conductivity media (e.g., $\sigma_e =$ 1mS/cm) than in high-conductivity media (4–5 mS/cm). This finding agrees with the earlier observations that a reduction of the ionic conductivity increases the uptake (or release) of various probe molecules induced by longer electric pulses (Kinosita & Tsong, 1977; Dimitrov & Sowers, 1990, Djuzenova et al., 1996). Low-conductivity media have also been found to facilitate the electrofusion of dielectrophoretically aligned cells (Stenger et al., 1991; Zimmermann & Neil, 1996; Zimmermann et al., 2000). Figure 3*B* reveals a critical value of the external conductivity $\sigma_e = 3$–4 mS/cm, above which the electrically induced uptake of PI was—if any—very low. Note that the "threshold" σ_e value matches well that of the cytosol of Sp2 cells $\sigma_i \approx 4$

mS/cm (Kürschner et al., 1998), and therefore corresponds to the condition at which the electrical stretching stress on the cell membrane vanishes ($P_D = 0$ if $\sigma_e = \sigma$, Eq. 6).

In the light of the above theoretical considerations our findings gave strong support for the assumption that the conductivity-dependent electrodeformation (i.e., elongation) force determined the degree of electropermeabilization of the plasma membrane upon a DC field pulse. This means that in the case of low-conductivity media, the electromechanical elongation stress acting on the cell membrane enlarges the breakdown area (in contrast to high-conductivity media), thus facilitating the uptake of the membrane-impermeable dye. Consistent with this conclusion, the experimental data (*open squares* in Fig. 3*B*) could be fitted quite accurately (*solid curve*) by using the equation for the electromechanical stress (Eq. 6) and the value of the cytosolic conductivity.

Applications of Ultra-Short Electric Pulses

The results presented here clearly demonstrate that ultra-short field pulses with the duration of 10–100 nsec can be used for the electroinjection of membrane-impermeable molecules into mammalian cells without significant loss of their viability. The large field strengths of up to about ~150 kV/cm required for membrane breakdown upon ultra-short pulses are easily available from the pulse power systems used here. Further applications of such high-intensity pulses might include the electropermeabilization of extremely small-sized cells and vesicles, such as bacteria, cell organelles, liposomes, etc. This is because both magnitude V_g and time constant τ_m of membrane-charging reduce linearly with decreasing cell radius a (Eqs. 1–3). Thus, in the case of a cell organelle (or vesicle) with a radius of 50 nm, τ_m is reduced to about 2 nsec and a critical field strength E_{crit} of ~135 kV/cm is necessary for membrane breakdown. Until now, the electropermeabilization with conventional pulse generators was performed on isolated cell organelles, e.g., to trigger the neurotransmitter release from secretory granules (Marszalek et al., 1997), or for introduction of DNA into mitochondria (Collombet et al., 1997). The fact that the plasma membrane of mammalian cells is capable of withstanding supracritical ultra-short field pulses (e.g., $E_0 > 100 \times E_{crit}$, Fig. 5) suggests the usefulness of the pulse systems described here for the in situ electropermeabilization of organelles within the cell without deterioration of the plasma membrane. As pointed out elsewhere (Collombet et al., 1997), the experimental techniques for the manipulation of the mitochondrial genome are essential for the analysis of molecular pathology and for therapy of a large group of mitochondrial disorders. Finally, the results of this study also show that low-conductivity media (i.e., whose conductivity is less than that of the cytosol) can greatly improve the electropermeabilization via the electrical stretching force exerted on the cell membrane.

We thank Willi Bauer, Marcus Behringer, Albert Gessner and Thomas Igerst for their skillfull assistance in manufacturing the nanopulsers. This work was supported by a grant from the Deutsche Forschungsgemeinschaft to UZ (Zi 99/12-1).

References

Benz, R., Beckers, F., Zimmermann, U. 1979. Reversible electrical breakdown of lipid bilayer membranes: a charge-pulse relaxation study. *J. Membrane Biol.* **48:**181–204

Collombet, J.M., Wheeler, V.C., Vogel, F., Coutelle, C. 1997. Introduction of plasmid DNA into isolated mitochondria by electroporation. A novel approach toward gene correction for mitochondrial disorders. *Biol. Chem.* **272:**5342–5347

Dimitrov, D.S., Sowers, A.E. 1990. Membrane electroporation—fast molecular exchange by electroosmosis. *Biochim. Biophys. Acta* **1022:**381–392

Djuzenova, C.S., Zimmermann, U., Frank, H., Sukhorukov, V.L., Richter, E., Fuhr, G. 1996. Effect of medium conductivity and composition on the uptake of propidium iodide into electropermeabilized myeloma cells. *Biochim. Biophys. Acta* **1284:**143–152

Engelhardt, H., Sackmann, E. 1988. On the measurement of shear elastic moduli and viscosities of erythrocyte plasma membranes by transient deformation in high frequency electric fields. *Biophys. J.* **54:**495–508

Friedrich, U., Stachowicz, N., Simm, A., Fuhr, G., Lukas, K., Zimmermann, U. 1998. High efficiency electrotransfection with aluminum electrodes using microsecond controlled pulses. *Bioelectrochem. Bioenerg.* **47:**103–111

Fuhr, G., Schnelle, Th., Müller, T., Hitzler, H., Monajembashi, S., Greulich, K.-O. 1998. Force measurements of optical tweezers in electro-optical cages. *Appl. Phys.* A **67:**385–390

Gift, E.A., Weaver, J.C. 2000. Simultaneous quantitative determination of electroporative molecular uptake and subsequent cell survival using gel microdrops and flow cytometry. *Cytometry* **39:**243–249

Heinz, V., Phillips, S.T., Zenker, M., Knorr, D. 1999. Inactivation of *Bacillus subtilis* by high intensity pulsed electric fields under close isothermal conditions. *Food Biotechnol.* **13:**155–168

Hofmann, F., Ohnimus, H., Scheller, C., Strupp, W., Zimmermann, U., Jassoy, C. 1999. Electric field pulses can induce apoptosis. *J. Membrane Biol.* **169:**103–109

Hyuga, H., Kinosita, K., Wakabayashi, N. 1991. Transient and steady-state deformations of a vesicle with an insulating membrane in response to step-function or alternating electric fields. *Jpn. J. Appl. Phys.* **30:**2649–2656

Isambert, H. 1998. Understanding the electroporation of cells and artificial bilayer membranes. *Phys. Rev. Lett.* **80:**3404–3407

Jeltsch, E., Zimmermann, U. 1979. Particles in a homogeneous electrical field: A model for the electrical breakdown of living cells in a Coulter counter. *Bioelectrochem. Bioenerg.* **6:**349–384

Jones, T.B. 1995. Electromechanics of Particles, Cambridge University Press, New York

Kinosita, K., Tsong, T.Y. 1977. Hemolysis of human erythrocytes by a transient electric field. *Proc. Natl. Acad. Sci. USA* **74:**1923–1927

Kinosita, K., Hibino, M., Itoh, H., Shigemori, M., Hirano, K., Kirino, Y., Hayakawa, T. 1992. Events of membrane electroporation vizualized on a time scale from microsecond to seconds. *In:* Guide to

Electroporation and Electrofusion. D.C. Chang, B.M. Chassy, J.A. Saunders, A.E. Sowers, editors. pp. 29–46. Academic Press, San Diego

Kononenko, V.L., Shimkus, J.K. 2000. Stationary deformations of erythrocytes by high-frequency electric field. *Bioelectrochem.* **52:**187–196

Kristiansen, M., Hagler, M.O. 1987. Pulsed power systems. *In:* Encyclopedia of Physical Science and Technology. Vol. 11. R.A. Meyers, editor. pp. 410–419. Academic Press, Orlando

Krueger, M., Thom, F. 1997. Deformability and stability of erythrocytes in high-frequency electric fields down to subzero temperatures. *Biophys. J.* **73:**2653–2666

Küchler, A. 1996. Hochspannungstechnik: Grundlagen—Technologie—Anwendungen. VDI Verlag, Düsseldorf

Kürschner, M., Nielsen, K., Andersen, C., Sukhorukov, V.L., Schenk, W.A., Benz, R., Zimmermann, U. 1998. Interaction of lipophilic ions with the plasma membrane of mammalian cells studied by electrorotation. *Biophys. J.* **74:**3031–3043

Lynch, P.T., Davey, M.R. 1996. Electrical Manipulation of Cells, Chapman & Hall, New York

Marszalek, P.E., Farrell, B., Verdugo, P., Fernandez, J.M. 1997. Kinetics of release of serotonin from isolated secretory granules. I. Amperometric detection of serotonin from electroporated granules. *Biophys. J.* **73:**1160–1168

Mussauer, H., Sukhorukov, V.L., Haase, A., Zimmermann, U. 1999. Resistivity of red blood cells against high-intensity, short-duration electric field pulses induced by chelating agents. *J. Membrane Biol.* **170:**121–133

Pawlowski, P., Fikus, M. 1989. Bioelectrorheological model of the cell. I. Analysis of stresses and deformations. *J. Theor. Biol.* **137:**321–337

Pethig, R., Markx, G.H. 1997. Applications of dielectrophoresis in biotechnology. *Trends Biotechnol.* **15:**426–432

Schoenbach, K.H., Peterkin, F.E., Alden, W.A., Beebe, S.J. 1997. The effect of pulsed electric fields on biological cells: Experiments and applications. *IEEE Trans. Plasma Sci.* **25:**284–292

Stenger, D.A., Kaler, K.V.I.S., Hui, S.W. 1991. Dipole interactions in electrofusion. Contribution of membrane potential and effective dipole interaction pressures. *Biophys. J.* **59:**1074–1084

Sukhorukov, V.L., Djuzenova, C.S., Frank, H., Arnold, W.M., Zimmermann, U. 1995. Electropermeabilization and fluorescent tracer exchange: the role of whole-cell capacitance. *Cytometry* **21:**230–240

Sukhorukov, V.L., Mussauer, H., Zimmermann, U. 1998. The effect of electrical deformation forces on the electropermeabilization of erythrocyte membranes in low- and high-conductivity media. *J. Membrane Biol.* **163:**235–245

Taylor, G. 1966. Studies in electrohydrodynamics. I. The circulation produced in a drop by an electric field. *Proc. Roy. Soc. (Lond.) A* **291:**159–166

Winterhalter, M., Helfrich, W. 1988. Deformation of spherical vesicles by electric fields. *J. Colloid Interf. Sci.* **122:**583–586

Zimmermann, U., Friedrich, U., Mussauer, H., Gessner, P., Hämel, K., Sukhorukov, V.L. 2000. Electromanipulation of mammalian cells: fundamentals and application. *IEEE Trans. Plasma Sci.* **28:**72–82

Zimmermann, U., Neil, G.A. 1996. Electromanipulation of Cells, CRC Press, Boca Raton, FL

Zimmermann, U., Pilwat, G., Riemann, F. 1974. Reversible dielectric breakdown of cell membranes by electrostatic fields. *Z. Naturforsch.* **29c:**304–305